



AIAA 2003-5345

Mechanization and Control Concepts for Biologically Inspired Micro Aerial Vehicles

David L. Raney
NASA Langley Research Center
Hampton, VA 23681-2199

Eric C. Slominski
Virginia Polytechnic Institute
Blacksburg, VA 24061

AIAA Guidance, Navigation & Control Conference
11-14 August 2003
Austin, Texas

For permission to copy or to republish, contact the American Institute of Aeronautics and Astronautics,
1801 Alexander Bell Drive, Suite 500, Reston, VA, 20191-4344.

Mechanization and Control Concepts for Biologically Inspired Micro Aerial Vehicles

David L. Raney*
NASA Langley Research Center
Hampton, VA 23681-2199

Eric C. Slominski†
Virginia Polytechnic Institute
Blacksburg, VA 24061

ABSTRACT

It is possible that MAV designs of the future will exploit flapping flight in order to perform missions that require extreme agility, such as rapid flight beneath a forest canopy or within the confines of a building. Many of nature's most agile flyers generate flapping motions through resonant excitation of an aeroelastically tailored structure: muscle tissue is used to excite a vibratory mode of their flexible wing structure that creates propulsion and lift. A number of MAV concepts have been proposed that would operate in a similar fashion. This paper describes an ongoing research activity in which mechanization and control concepts with application to resonant flapping MAVs are being explored. Structural approaches, mechanical design, sensing and wingbeat control concepts inspired by hummingbirds, bats and insects are examined. Experimental results from a testbed capable of generating vibratory wingbeat patterns that approximately match those exhibited by hummingbirds in hover, cruise, and reverse flight are presented.

INTRODUCTION

With numerous civil and military applications, micro-aerial vehicles (MAVs) represent an emerging sector of the aerospace market, and may one day become quite commonplace. The Defense Advanced Research Projects Agency (DARPA) has generally defined the MAV as a class of aircraft with a maximum dimension of 6 inches that is capable of operating at flight speeds of approximately 25 mph or less, with a mission duration of 20 to 30 minutes.¹ A concerted effort supported by DARPA has resulted in advancements in miniaturized digital electronics, low Reynolds number aerodynamics, multidisciplinary design methods and other enabling systems technologies for MAVs. Such advances have turned the concept of a tiny autonomous flight vehicle for use as a rapidly deployable eye-in-the-sky from fiction into demonstrated fact.² Continual reductions in the size, weight and power consumption of video and other sensing devices are improving the feasibility of

MAVs for use as inexpensive and expendable platforms in surveillance and data collection missions where larger vehicles are not practical.

A number of successful fixed-wing MAV designs have been generated by several university, commercial, and government-funded endeavors. Examples shown in Figure 1 include Aerovironment's *Black Widow*, the *Trochoid* developed by Steve Morris of MLB, and a flexible-wing design by the University of Florida.³⁻⁵ The unique wing structure of the UF design incorporates a highly flexible battened membrane concept inspired by sail technology. The structure consists of a carbon-epoxy composite frame that is covered with a thin layer of latex, and is somewhat reminiscent of a bat wing.⁶ Waszak has investigated the aeroelastic deformation of this wing structure in a series of wind tunnel tests, and a dynamic simulation model of the UF MAV design has been created for use in flight control law development.^{7,8}

Numerous civil and military applications for MAVs have been proposed, and far more have yet to be imagined. However, the potential applications of current fixed-wing designs are necessarily limited due to maneuver constraints. The successful fixed-wing designs mentioned above rely on relatively conventional scaled-down aerodynamics and flight control approaches, and they do not possess the flight agility and versatility that would enable missions such as rapid flight beneath a forest canopy or within the confines of a building. In order to perform missions requiring extreme agility, MAV designs of the future may exploit flapping flight. The ability to vary wingbeat kinematics to generate large control moments and to rapidly transition between flight modes is a hallmark of nature's most agile fliers.

Although a number of flapping mechanisms have been developed and demonstrated in a limited fashion, the creation of a practical ornithoptic MAV remains an elusive goal. Mechanical design, efficient actuation, power systems and control pose significant challenges to the feasibility of an ornithoptic MAV concept. As a

* Research scientist, Dynamics and Control Branch, Member AIAA.

† Graduate Student, Mechanical and Aerospace Engineering Department, Member AIAA



Figure 1. Several successful fixed-wing MAVs, from left to right, Aerovironment's *Black Widow*, MLB's *Trochoid*, and the University of Florida's flexible wing design.

means of efficiently generating high-frequency flapping motions, many natural flyers generate lift through resonant excitation of an aeroelastically tailored structure: muscle tissue is used to excite a structure which exhibits a particular vibratory mode shape that generates propulsive lift.⁹⁻¹¹ Several research endeavors have considered MAV concepts that would operate in a similar fashion.¹²⁻¹⁴ Related research activities span a broad range of disciplines including ornithology, entomology, structures, materials, sensing, unsteady fluid dynamics and control. An extensive review of biological and aeronautical literature relevant to flapping flight was provided by Shyy¹⁵, and a highly multidisciplinary conference on low Reynolds number fixed and flapping-wing flight was held at Notre Dame in 2000.¹

Shown in Figure 2 are a number of flapping MAV concepts including Aerovironment's *Microbat*, Vanderbilt's *Elastodynamic Ornithoptic Robotic Insect*, and UC Berkeley's *Micromechanical Flying Insect*. The *Microbat* was designed by Aerovironment in partnership with UCLA and Caltech under funding from DARPA.¹⁶ To create *Microbat*, the team drew upon advancements in microstructures, miniature electronics, unsteady fluid dynamic modeling and multidisciplinary design optimization. The vehicle was capable of brief radio-controlled flights, and its limitations provided great insight in terms of necessary directions for follow-on research activities.

However, one of the keys to agility in flapping flight is the ability to vary the wingbeat kinematics. The *Microbat* lacked this degree of control, relying instead on

a conventional tail and rudder arrangement to provide flight control functions. One of the goals of the current investigation was to explore a more biologically inspired realization of the flapping wing apparatus that could afford some degree of control over the wingbeat kinematics.

Also pictured in Figure 2 is a concept for an *Elastodynamic Ornithoptic Robotic Insect* that was studied by Frampton and Goldfarb at Vanderbilt.¹⁷ The concept involved the mechanical amplification of small displacements produced by piezoceramic wafer actuators to excite vibrating wing structures. The investigators performed a parametric study of the impact of various combinations of bending and torsional wing stiffness on the thrust production of flapping wings.

Perhaps the most multidisciplinary effort to create an ornithoptic MAV is being undertaken by the *Micromechanical Flying Insect* design team at UC Berkeley. This team is responsible for an impressive series of biological and engineering studies aimed at understanding natural insect fliers in the size range of 2.5cm, and designing an artificial system capable of emulating that behavior.^{18,19} A key element of their research addresses the manner in which insects adjust the phasing between flapping and rotational motions of their vibrating wing structures for the purpose of flight control.

This paper describes an ongoing research activity in which resonant flapping MAV concepts are being explored in a small project at NASA Langley Research Center. The study targets a MAV size range of 15-20cm.

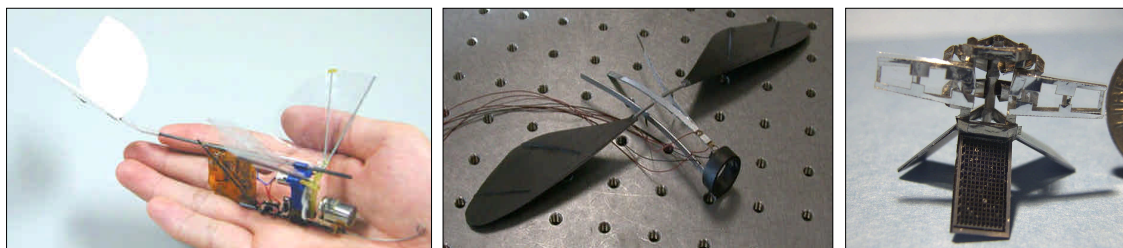


Figure 2. Several ornithoptic MAV concepts, from left to right, Aerovironment's *Microbat*, Vanderbilt's *Elastodynamic Ornithoptic Robotic Insect*, and UC Berkeley's *Micromechanical Flapping Insect*.

The research does not seek to develop a flapping MAV design, nor prove the feasibility of such an ornithoptic system.[§] Rather, the goal is to develop insight regarding biologically-inspired structural approaches, mechanical arrangements, actuation concepts, sensing, and wingbeat control approaches that could contribute to the body of knowledge required to create an agile MAV in which resonant excitation of an aeroelastically tailored wing structure is used to generate propulsive lift.

First, several insights and specifications are drawn from biological inspirations for flapping MAVs. A structural concept that was applied to create wings having size, weight and planform similar to that of a particular hummingbird example is then described. Next, a biologically inspired arrangement of mechanical components is developed to provide control over vibratory wingbeat patterns, and results from a vibratory testbed apparatus are presented. A feedback control circuit is described that automatically tunes the actuation drive signal to the resonant flapping frequency of the flexible wing structures. A simple means of varying the actuator signals to generate wingbeat patterns that approximately match those exhibited by hummingbirds in hover, cruise, and reverse flight is also presented.

BIOLOGICAL INSPIRATION FOR AN ORNITHOPTIC MAV

Although numerous examples of highly successful flapping fliers exist in nature, perhaps the one that best demonstrates the characteristics we wish to possess in an agile MAV is the hummingbird. Hummingbird species bracket the size range of 6 inches and speed range of 25 mph, used to define MAV-class vehicles. Wing lengths range from about 33 mm (~2.5" total span) for one of the smallest species (*Calliphlox amethystina*), to 135 mm (~10.5" total span), for the Giant Andean (*Patagona gigas*). Wind tunnel tests have revealed maximum flight speeds as high as 27 mph for some species, compared to 8 to 10 mph for most fast-flying insects.²¹

The agility, precision, and flight mode variability exhibited by hummingbirds is astonishing, and the creation of an artificial system that can perform similarly is a lofty goal. Precise control of body axis rotation and translation during hover feeding is a necessity for hummingbirds. Transition from hover to cruise may be accomplished in less than half a second, incurring accelerations of roughly 5-gs. Despite their relatively high power consumption during hovering flight, hummingbirds are able to cruise with considerable efficiency, and some species migrate across the Gulf of Mexico without feeding.

[§] Such proof clearly exists in the form of natural fliers. At issue, however, are the relative merits of rotary vs. flapping approaches to MAV flight. Spedding examines this topic.²⁰

In terms of size, weight, and Reynolds number, hummingbirds occupy a niche between insects and larger birds, and their flight apparatus appears to represent a hybrid between the two approaches to flapping flight. Many insects employ a flight apparatus that relies upon resonant excitation of a relatively passive wing structure to produce a vibratory response that generates propulsive lift. Most birds, on the other hand, rely on highly articulated wing structures that move at the elbow and wrist as well as the shoulder joint. Their wingbeat kinematics are generally more complex, involving variation of the wing planform geometry throughout the flapping cycle. Although birds tend to flap their wings at the natural frequency of their biomechanical system, their highly articulated flapping motions cannot be fully described merely as the vibratory response of a passive structure. This additional degree of complexity would seem to endow birds with generally broader flight envelopes and greater variability of function in terms of flight modes and behaviors.

Although the morphology of the hummingbird flight apparatus is distinctly avian, its mode of operation bears a strong resemblance to insects. Unlike all other flying birds, a hummingbird's wing joints are fused at the elbow and wrist, so the wing planform does not change during the flapping cycle.²¹ Flapping motions are actuated entirely from the shoulder joint, and wingbeat kinematics of the upstroke and downstroke are markedly similar. The wing exhibits a vibratory motion much like that of an insect wing: a non-articulated structure that is aeroelastically tailored to generate propulsive lift when excited at resonance. The relative simplicity of the hummingbird's flight apparatus and wingbeat patterns, together with its remarkable precision and flight mode variability, make it an attractive source of inspiration for mechanization and control concepts that may be applied to an agile ornithoptic MAV.

In order to use the hummingbird as source of further insight, it makes sense to develop specifications that characterize those species in the size range of interest. A study by researchers at the University of Texas that investigated the load carrying capacity of several hummingbird species provides a useful starting point.²² Average characteristics for these species are presented in Table 1 from the study by Chai and Millard, which also provides an assessment of wing and flight muscle mass. Note the wingbeat frequencies ranging from 23.3 Hz to 51.7 Hz. Approximate wingbeat frequencies for all hummingbird species range from 10 Hz (*P. gigas*) to 80 Hz (*C. amethystina*).²¹ Parameters P_{per} and P_{zero} in the table represent total mechanical power output of the flight muscle mass assuming perfect and zero elastic energy storage, respectively.

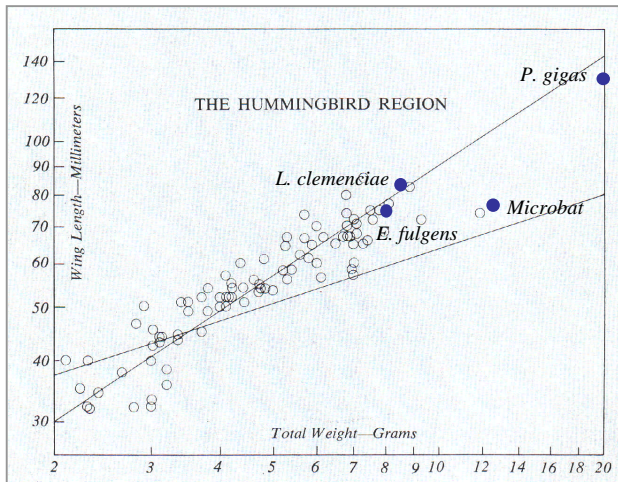
	<i>Lampornis clemenciae</i>	<i>Eugenes fulgens</i>	<i>Archilochus alexandri</i>	<i>Selasphorus rufus</i>
total mass, g	8.4	7.4	3.0	3.3
wing mass, g	0.29	0.26	0.08	0.08
flt muscle mass, g	2.44	2.01	0.87	0.96
wing AR	8.2	8.4	7.1	7.4
freq, Hz	23.3	24.0	51.2	51.7
length, mm	85	79	47	42
flap arc, deg	151	150	126	163
U_t , m/s	10.4	9.9	10.5	12.3
Re	11400	9800	7400	7400
C_L	1.46	1.67	1.42	1.41
P_{per} , Watt	0.175	0.152	0.076	0.089
P_{zero} , Watt	0.343	0.325	0.187	0.250
$f l^{5/4}$	6014	5653	6301	5528
$m/l^{3/2}$	0.0107	0.0105	0.0093	0.0121

Table 1. Data for several hummingbird species.²²

Two species that lie within the relevant size range are the Blue Throat (*Lampornis clemenciae*), and the Rivoli (*Eugenes fulgens*). These species are highlighted on the plot of wing length vs. total weight shown in Figure 3 for all hummingbird species. Also noted on this plot is Aerovironment's ornithoptic MAV design, the *Microbat*. An empirical fit to the hummingbird data suggests that weight scales with wing length according to the relation shown in equation (1).²¹ Greenwalt also suggests that hummingbird wing length and flapping frequency scale according to equation (2).

$$m \propto l^{3/2} \quad (1)$$

$$f \propto l^{-5/4} \quad (2)$$

Figure 3. Plot of wing length vs. total weight for all hummingbird species.²¹

Using values of mass, wing length, flapping frequency and flapping arc from Table 1 to compute average scale factors from these relations, it appears that a hummingbird-like MAV with wing length of 75 mm should flap its wings through a 150-degree flapping arc at approximately 25 Hz and weigh only 7.5 grams. The

weight target for this conceptual vehicle represents an extreme challenge to the various subsystem technologies of structures, power systems, actuation and miniaturized electronics. The realization of an artificial MAV with truly bird-like agility would seem to hinge upon the development of such ultra-lightweight components. However, it is not only the availability of suitable system components, but the particular arrangement and manner in which they are employed that will lead to a MAV with the desired capabilities. The following sections present concepts for mechanization and control of a vibrating wing apparatus that could provide lift, thrust, and maneuver moments for such a MAV if and when the necessary component technologies emerge.

STRUCTURAL CONCEPT FOR FLEXIBLE WINGS

To produce artificial wing structures with the desired flexible characteristics, a structural concept was adapted from the UF MAV design shown in Figure 1. Although it employs a fixed-wing and propeller arrangement, this vehicle incorporates a bat-like flexible membrane wing structure that is thought to provide improved stall margins and handling characteristics. The wing is constructed from a carbon-epoxy composite frame that is covered with a thin latex membrane.⁶ For the present investigation, this structural concept was applied to wing designs inspired by hummingbirds. Wing layouts were developed from photographs of hummingbirds with their wings extended that were scaled to have a single-wing length of 75 mm. An example of the resulting composite wing structure is shown in Figure 4, along with the photograph from which it originated. The weight of the composite wing structure is 0.59 grams, compared to 0.26 grams for a natural wing of similar size from Table 1. Several features in the structure of the hummingbird wing appear important to capture in the artificial wing design.

First, the quills of the primary flight feathers radiate from the shoulder region of the wing, rather than emanating from the leading-edge spar as in the University of Florida MAV. Radial orientation of structural wing members is a key element observed in natural fliers, and it has been found to greatly influence the flexible behavior of their wings. A description of the crucial role that such orientation plays in the resulting torsional dynamics of insect wings is provided by Ennos.²³ In the hummingbirds' case, the radial orientation of quills provides the flexible wing with partially reversible camber, enabling it to generate lift on both the downstroke and upstroke segments of the flapping cycle during hovering flight, in which the stroke plane is nearly horizontal. This reversible characteristic of the wing is highly developed in hummingbirds, as illustrated by the hovering specimen shown in Figure 5.²¹

Among avian species, hummingbirds possess proportionately the largest flight musculature associated with the rearward portion of the flapping stroke. The reversibility of their flexible wing structure along with their unusual flight musculature is largely responsible for the hummingbird's prowess as a hovering flier.

Another critical feature required to generate the flexible behavior observed in Figure 5 is a wing surface that is capable of supporting compound curvature without puckering. The extensible compliant latex material used in the flexible wings of the University of Florida MAV has been shown in wind-tunnel tests to be capable of supporting such deformations.⁷

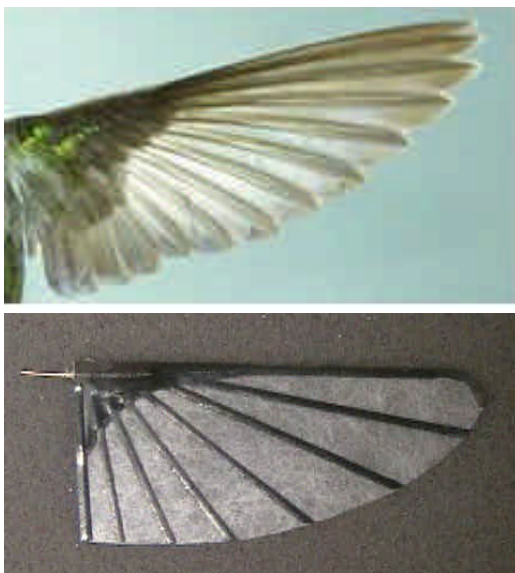


Figure 4. Extended hummingbird wing and a typical wing created by applying UF structural concept to hummingbird-inspired wing designs.



Figure 5. A hummingbird in hovering flight illustrates the reversible camber exhibited by its flexible wing structure (*Eutoxeres aquila*).²¹

GENERATION OF VIBRATORY FLAPPING MOTION

If the motivation for pursuit of a flapping flight mechanism is bird-like agility, then a crucial goal is to provide some degree of control over the wingbeat kinematics as a means of changing flight modes or generating maneuvers. In order to achieve variability in wingbeat behavior, a vibratory flapping system was designed that includes a ball and socket joint at the shoulder. The design of the system represents an attempt to apply insights from the basic arrangement of skeletal and muscular components that drive a typical bird wing shown in Figure 6, which is drawn from Freethy, 1982.²⁴ The storage of elastic energy has been found to be an important factor in the arrangement and operation of this system. We shall drastically simplify and then crudely model these components as an elastodynamic system, while attempting to retain the basic function of the arrangement. The simplified mechanical system shown in Figure 7 provides a basis for development of the model. The following paragraphs describe the various components and the rationale for their arrangement.

In Figure 6, a ball-and-socket joint connects the coracoid to the humerus, constituting the shoulder of the bird. At point h in Figure 7, this component is represented as a 3-degree of freedom ball-and-socket connection between a fixed rigid test stand and a rigid beam element having length L_1 and mass m , representing the humerus. The use of a rigid beam element in this capacity means that the flexible dynamics of the wing structure itself are neglected for the time being.

Two reference frames are defined consisting of body-fixed axes $\{b\}$ and wing-fixed axes $\{a\}$, both having their origin at the shoulder joint, h . Control over the relative amplitude and phasing of angular rates of rotation between these two coordinate systems will enable the arrangement to generate changes in the vibratory wingbeat pattern. (The shoulder joint of insects is also designed to permit such control, but the insect's shoulder anatomy resembles a series of hinges that has been compared to the articulated rotor hub of a helicopter.²⁵ It differs markedly from the ball-and-socket shoulder joint found in birds.)

Located distance L_2 from the shoulder joint h is the application point, f , for a pair of tendons that connect the beam element to points c and d , which represent the attachments of the depressor muscle, *pectoralis*, to the sternum and scapula in Figure 6, respectively. The tendons are able to contract, thereby generating forces F_1 and F_2 that act upon the beam at point f . In Figure 6, the pectoralis muscle serves to draw the wing down through a stroke plane having an inclination to the bird's body axis that may be varied by changing the relative magnitudes of muscular contraction that generate the

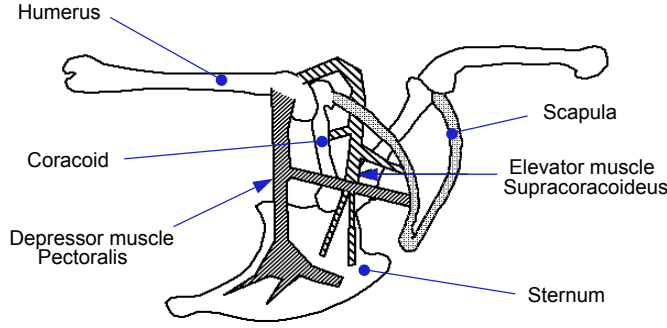


Figure 6. Basic arrangement of skeletal and muscular components comprising the avian flapping system.²⁴

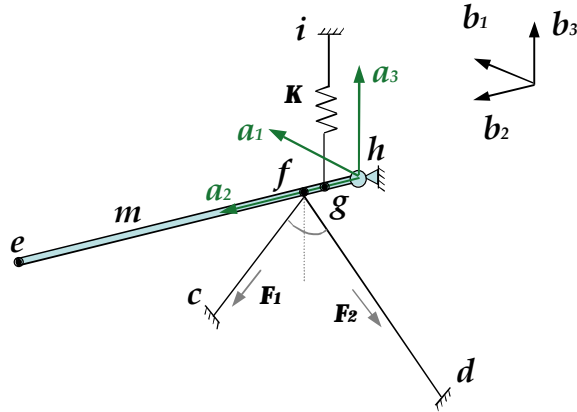


Figure 7. Simplified arrangement of mechanical components used to approximate the natural system shown in Figure 6.

sternum-humerus and scapula-humerus resultant forces. As a simplification in the model, these tendons attach to the beam at equal and opposite angles to the a_2 - a_3 plane with magnitude .

Located a distance L_3 from the shoulder joint is the attachment point, g , for a vertical spring that represents the elevator muscle, *supracoracoideus*, which raises the wing. The justification for representing this muscle with a single spring element is that the *supracoracoideus* passes through a small notch that permits it to travel around and over the top of the coracoid before reversing direction and attaching to the sternum, as shown in Figure 6. This notch constrains the line of action of the elevator muscle to pass through a point at the top of the coracoid, much as the force generated by the spring shown in Figure 7 acts through point i . The use of the spring element collectively represents the elastic storage potential that has been attributed to the sternum and scapula arrangement.

SIMULATION MODEL

A simulation model of the mechanical arrangement shown in Figure 7 was programmed in MatlabTM to evaluate the potential for the system to generate wingtip

trajectories similar to those exhibited by hummingbirds. Using notation from Smith (1996),²⁶ two reference frames are defined consisting of body-fixed axes $\{b\}$ and wing-fixed axes $\{a\}$, both having their origin at the shoulder joint, h . The body axis system $\{b\}$ represents an inertial frame of reference fixed to the stationary test stand. In order to predict wingtip trajectories the simulation must generate time histories for the vector r_e^b , relating the position of tip of the rod, e , in the body-fixed coordinate system $\{b\}$. This vector is given by:

$$r_e^b = [T_{ab}]^T r_e^a$$

Where r_e^a is the position of e in the wing-fixed coordinate system $\{a\}$, given by $r_e^a = [0 \ L_1 \ 0]^T$. The Euler angle rotation sequence $(\psi \ \theta \ \phi)$ relates the coordinate systems $\{a\}$ and $\{b\}$ via the direction cosine matrix T_{ab} such that $\{a\} = T_{ab} \{b\}$ where:

$$T_{ab} = \begin{bmatrix} \cos \theta \cos \psi & \cos \theta \sin \psi & -\sin \theta \\ \sin \phi \sin \theta \cos \psi - \cos \phi \sin \psi & \sin \phi \sin \theta \sin \psi + \cos \phi \cos \psi & \sin \phi \cos \theta \\ \cos \phi \sin \theta \cos \psi + \sin \phi \sin \psi & \cos \phi \sin \theta \sin \psi - \sin \phi \cos \psi & \cos \phi \cos \theta \end{bmatrix}$$

The Euler rotations $(\psi \ \theta \ \phi)$ are respectively referred to as folding, feathering and flapping in describing the wingbeat kinematics of natural fliers. The kinematic differential equations relating the Euler angle rates and the angular rotation rates $(p \ q \ r)$ of $\{a\}$ relative to $\{b\}$ are:

$$\begin{aligned} \dot{\phi} &= p + (q \sin \phi + r \cos \phi) \tan \theta \\ \dot{\theta} &= q \cos \phi - r \sin \phi \\ \dot{\psi} &= (q \sin \phi + r \cos \phi) / \cos \theta \end{aligned}$$

Several assumptions serve to simplify the simulation. First, representation of the humerus with a rigid homogenous beam element having shoulder joint, actuator and spring attachment points all lying along the centerline means that the feathering degree of freedom is neither driven by actuator inputs nor excited by inertial coupling. Furthermore, let the mechanical attachment at point f be defined such that feathering motion of the beam is prohibited. Thus $\dot{\theta}$ is identically zero, implying $q = r \tan \theta$.

Having eliminated the \dot{q} equation by a kinematic constraint, the remaining portion of the moment equation may be written as:

$$J \begin{bmatrix} \dot{p} \\ \dot{r} \end{bmatrix} = M_A + M_R + M_D$$

where J is the inertia matrix having diagonal elements equal to $(mL_1^2)/4$ and M_A , M_R , and M_D respectively represent moments due to actuating forces, restoring forces, and damping acting on the beam. Moments arising from actuator force inputs are given by:

$$M_A = \begin{bmatrix} -L_2 \cos \lambda \cos \phi & -L_2 \cos \lambda \sin \phi \\ -L_2 \sin \lambda \cos \psi & L_2 \sin \lambda \sin \psi \end{bmatrix} \begin{bmatrix} F_1 \\ F_2 \end{bmatrix}$$

where F_1 and F_2 are time varying force inputs generated by linear actuators located at points c and d in Figure 7. Moments arising from restoring forces provided by the spring are given by:

$$M_R = \frac{\sin\phi \cos\phi}{\sin\psi} \left\{ -KL_3^2 \right\}$$

Moments arising from aerodynamic damping and friction of the shoulder joint are expressed as:

$$M_D = \begin{bmatrix} C_1 & 0 \\ 0 & C_2 \end{bmatrix} \begin{bmatrix} p \\ r \end{bmatrix}$$

where C_1 and C_2 are estimated constants. As a further simplification, attachment points f and g for the spring and actuator tendons representing the elevator and depressor muscles were co-located, so $L_2 = L_3$. Values were chosen for L_1 and m based on the actual composite wing length and weight. A tendon attachment location, L_2 , and spring constant, K , necessary to produce a natural frequency of 25 Hz were then selected where:

$$\omega_n = \frac{L_2}{0.5L_1} \sqrt{\frac{K}{m}}$$

The simulation was implemented in Matlab's Simulink™ with a step size of 1ms using the ODE4 (Runge-Kutta) integration solver with the following parameter values: C_1 & $C_2 = 10e^{-5}$ N/cm/s, $L_1 = 7.5$ cm, L_2 & $L_3 = 0.5$ cm, $K = 8.19$ N/cm, $m = 0.59$ gm, $\lambda = 40$ deg.

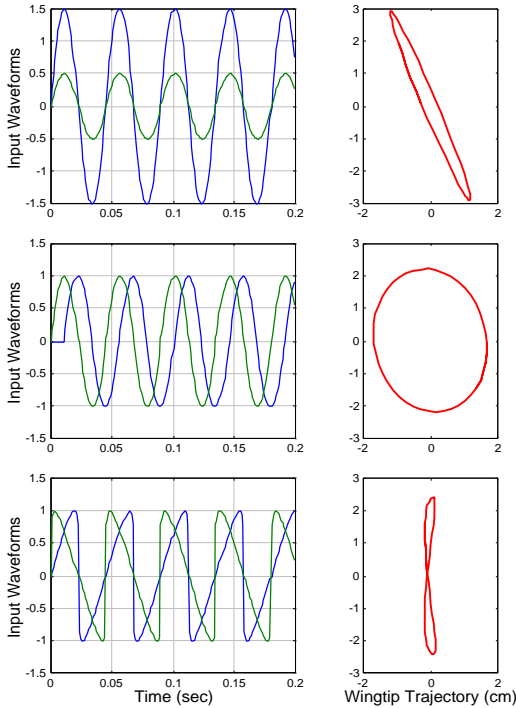


Figure 8. Example waveforms used to control vibratory wingtip trajectory produced by the dynamic simulation.

By providing periodic inputs F_1 and F_2 at the resonant flapping frequency of 25 Hz, the element representing the wing humerus can be made to undergo a large-amplitude vibratory flapping motion. Factors that affect the relative amplitude, phasing, and waveform of F_1 and F_2 can be used to control various aspects of the wingtip trajectory. Examples of actuator input waveforms and resulting wingtip trajectories are shown in Figure 8.

VIBRATORY TESTBED APPARATUS

Based on the promising simulation results, a vibratory flapping apparatus was constructed using the biologically inspired component arrangement from Figure 7. The goal was to create a benchtop testbed capable of generating vibratory wingbeat patterns similar to those observed in hummingbirds. Dispensing with component weight limitations levied by the need for a flight-capable design led to the testbed shown in Figure 9. A crucial component of the apparatus is the 3-dof pinned ball-and-socket used for the shoulder joint. This joint permits a limited range of feathering and folding rotations, and unconstrained flapping rotation. The pinned ball-and-socket was resorted to after attempts with a true ball-and-socket repeatedly resulted in the ball departing from the socket when the system was excited at resonance. Nylon line connects the main spar of the wing, representing the humerus, to two linear actuators that provide input forces F_1 and F_2 , representing the pectoralis. Two Labworks ET-126A electrodynamic linear shaker actuators driven by Labworks PA-138-1 power amplifiers were used in this capacity. The supracoracoides was represented by a spring that was attached to a point 10.5 cm above the shoulder joint. The flexible wing structure, itself, consisted of the carbon prepreg and latex composite described previously.

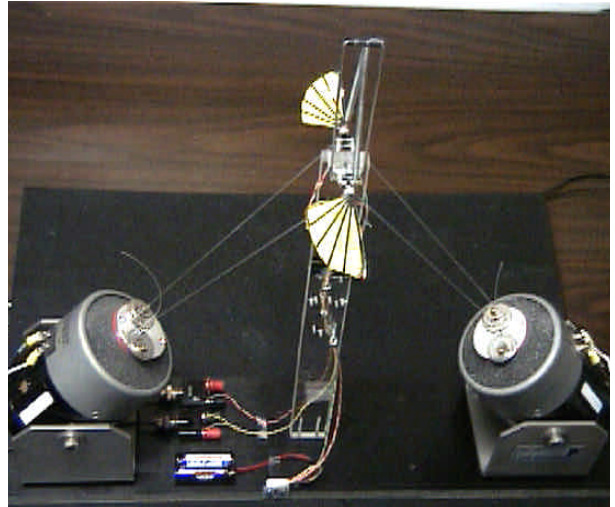


Figure 9. Shaker-actuated testbed designed to provide control of vibratory wingbeat patterns.

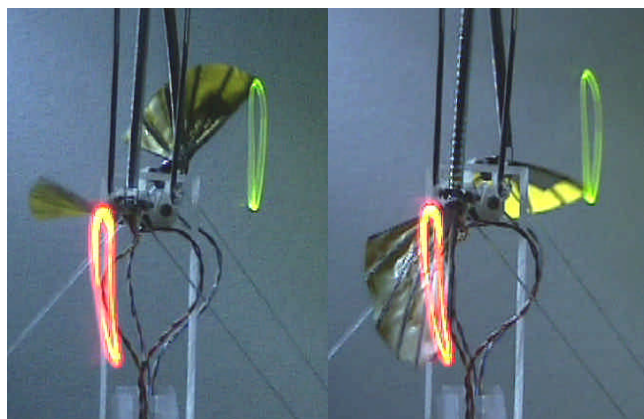


Figure 10. Strobed photographic images illustrating vibratory flapping motion and wingtip trajectories traced out by LEDs at resonant wingbeat frequency ($\sim 25\text{Hz}$).

Several experimental techniques have proven useful in assessing the performance of this apparatus. The first is the use of a tunable strobe light, which permits the creation of an aliased slow-motion video image of the high frequency periodic motion. The use of the strobe greatly improves the ability to qualitatively assess the behavior of the flexible wing structure. Another effective technique is the placement of small LED devices at the tips of the wings to trace out the entire wingtip trajectory in a single photographic image. By combining these methods, it is possible to generate images that illustrate the large-amplitude vibratory flapping motion of the wings at resonance, as shown in Figure 10.

As in the dynamic simulation model, control inputs to the apparatus consist of scale factors on the relative amplitude, phasing and waveform of commands to the two electrodynamic actuators. These provide a degree of control over the wingtip trajectory, enabling the system to approximate wingbeat patterns exhibited by hummingbirds in various flight modes. A comparison of wingtip trajectories produced by the testbed with hummingbird wingtip trajectories documented by Greenwalt is shown in Figure 11. The factors that are approximately matched in these figures include the stroke plane inclination to the body axis of the bird (or testbed), amplitude of the flapping arc, approximate geometry of the wingtip trajectory, and sense of rotation about that trajectory. Note that in forward flight, the wing travels clockwise about the trajectories shown in Figure 11, while in reverse flight the wing travels in a counter-clockwise sense. Transition between wingbeat patterns has been accomplished in as little as four flapping cycles (0.16 seconds). These results suggest that the biologically inspired mechanical arrangement in Figure 7 provides sufficient control over the vibratory wingbeat pattern to enable the flight mode variability that would be required by an agile ornithopter MAV.

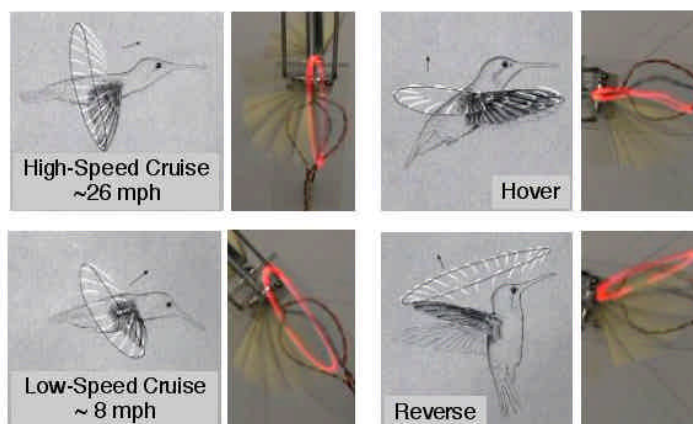


Figure 11. Comparison of wingtip trajectories produced by the vibratory flapping testbed with those exhibited by hummingbirds in various flight modes.²¹

The apparatus provides control over the wingtip trajectory as defined by a particular combination of folding and flapping motions. However, the feathering component of the vibratory wing motion produced by the testbed is uncontrolled. Many insects use the phasing between feathering and flapping motions as a steering mechanism, implying some degree of control over feathering rotations via moments generated at the shoulder joint.¹⁸ But entomologists have also found that insects rely heavily upon inertial and aerodynamic loading to affect rotation of the wing.²⁷ The degree to which hummingbirds exercise direct actuation and control of wing feathering rotations for steering purposes is uncertain. Although the feathering rotation is not directly actuated or controlled in the current mechanical arrangement, some degree of control may be achieved by introducing offsets between various tendon attachment points at the humerus in Figure 7. This is a topic for further research.

It is important to distinguish between wing torsion and feathering motions. The former refers to structural deformation of the wing about the torsional axis, while the latter is the rigid-body component of wing rotation about the a_2 axis. A similar distinction exists for bending and flapping components of wing motion. It is clear from Figure 10 that the experimental wing undergoes considerable bending and torsion at resonance. This behavior is strongly influenced by the stiffness distribution of the wing lay-up (dictated by ply number, membrane thickness, and dimensions of composite members.) Ideally, a prescribed mode shape, consisting of a particular combination of wing bending and torsion that has been tuned to generate propulsion and lift, would be designed into the wing structure at the desired resonant frequency by appropriately tailoring the composite lay-up. Aeroelastic tailoring of the wing structure is another topic for further research.

CONCEPT FOR RESONANT TUNING

A means of sensing the flexible behavior of the vibrating wing structure was found in the form of thin film piezoelectric strain rate sensors made of polyvinylidene fluoride (pvdf). These commercially available sensors, manufactured by Measurement Systems, Inc. (MSI), employ the piezo effect to produce a voltage output in response to strain rate. The thinnest devices available consist of a $28\mu\text{m} \times 15\text{mm} \times 40\text{mm}$ layer of “metalized” pvdf material. These sensors are easily bonded to the composite wing structure using a thin coat of spray adhesive, as shown in Figure 12. In this arrangement the sensor responds to a broad range of deformations, including the overall bending and twisting motions of the wing as well as individual batten and membrane vibrations. The voltage output of the sensor was found to be easy to use and quite repeatable. Sensors were applied to both wings of the testbed apparatus.

An RMS sensor output signal may be computed to provide a gross indication of the amplitude of vibration the flexible wing experiences at a given excitation frequency. It is then possible to experimentally ascertain the fundamental resonant flapping frequency of the wing structure by conducting an input frequency sweep and plotting RMS sensor output against input frequency. Such a plot is shown in Figure 13 for a flexible wing structure that resonates at approximately 24 Hz.

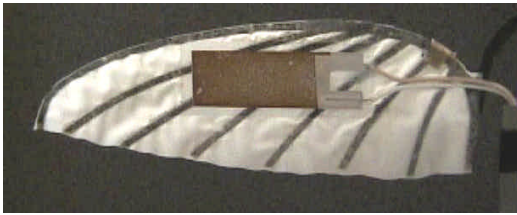


Figure 12. Thin film pvdf strain-rate sensor device bonded to flexible wing structure.

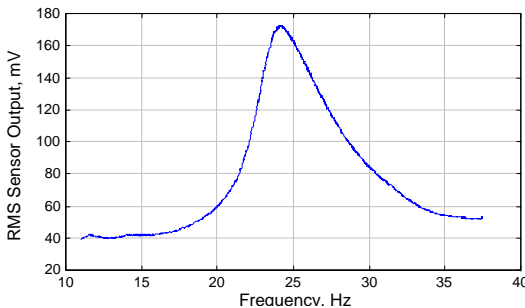


Figure 13. Plot of the RMS strain-rate sensor output vs. input frequency showing resonant peak at 24 Hz.

The frequency response plot suggests the potential for a feedback control circuit that would automatically tune the actuator input frequency to the resonant frequency. The inspiration for such a tuning circuit

derives from a recent text on the biomechanics of insect flight by Dudley.⁹ This reference notes that certain dome-shaped sensory organs (*campaniform sensillae*) identified within the structure of locust wings have been found to respond specifically to wing deformation. These organs tend to be concentrated near the base of the wings, where bending is greatest. Feedback signals from these “stretch receptors” are used to drive the primary flight musculature within in the locust’s body. Such feedback *directly stimulates and phase-locks thoracic motor neurons at the wing oscillation frequency*. In fact, the vibratory motion of the wing itself is both necessary and sufficient to generate the neural stimulus to the muscle tissue that sustains the oscillation. Hence, the biomechanical vibratory system simply contains neuromuscular feedbacks from the flexible wing structure that cause it to operate at resonance when activated.

It is possible to devise a feedback circuit that employs the thin film strain rate sensor in a capacity similar to that of the locust’s campaniform sensillae. The simplicity of deriving such a circuit becomes obvious upon consideration of the forced response of a 2nd order system with positive rate feedback:

$$\ddot{\eta} + 2\zeta\omega_n\dot{\eta} + \omega_n^2\eta = F \quad (4)$$

let $F = G\dot{\eta}$

$$\ddot{\eta} + (2\zeta\omega_n - G)\dot{\eta} + \omega_n^2\eta = 0 \quad (5)$$

Let η represent the generalized modal coordinate for the first bending mode shape of the wing, and the rate signal, $\dot{\eta}$, represent output of the strain rate sensor (an idealization which assumes that the sensor responds only to the first bending mode of the structure). Let F represent a generalized force input to the wing structure that is generated by a command to the electrodynamic actuators under the condition $F_1 = F_2$. Setting the forcing function equal to feedback gain, G , times the strain rate sensor output, $\dot{\eta}$, yields equation (5). The linear system is dynamically unstable for sufficiently high feedback gain, $G > 2\zeta\omega_n$, resulting in a divergent oscillation of the vibrating structure. However, insertion of a saturation nonlinearity on the strain-rate feedback signal prior to multiplying by gain G , causes the system to exhibit a limit-cycle oscillation at the resonant frequency of the 2nd order system, rather than a divergence. The saturation represents a limit on the power used to drive actuators, preventing the force input from increasing without bounds. The amplitude of the limit cycle may be controlled by varying G , which is equivalent to scaling the power used to drive the actuators. Increasing G results in greater flapping amplitude, generating greater propulsive lift while maintaining the same flapping frequency – a convenient throttle control for the resonant flapping system.

This resonant tuning circuit was implemented for the vibratory test stand using dSpace™ hardware-in-the-loop simulation equipment. A predictable obstacle was encountered as a result of a basic assumption employed in the preceding development: the output of the strain rate sensor does not only represent the derivative of the first bending mode generalized coordinate (which constitutes the fundamental flapping motion we wish to excite). Instead, the signal also includes higher frequency contributions from batten and membrane vibratory modes. As a result, the closed-loop system performs unpredictably, often tuning to a much higher frequency than desired. Examination of the signal from the strain rate sensor revealed that, although there did indeed appear to be considerable high frequency content, the predominant signal content reflected the fundamental bending mode. The result was that zero crossings of the signal occurred at the frequency of the fundamental mode. Such an outcome is greatly influenced by the orientation of the sensor relative to wing the structure. If the sensor is positioned to respond predominantly to the fundamental bending mode, then it is likely that zero crossings may provide an indication of the fundamental mode frequency for the tuning circuit.

To examine this possibility, the feedback portion of the block diagram was changed to a simple scalar factor on the sign of the strain rate signal, resulting in a square wave at a frequency that depends solely on the zero crossing of the strain rate sensor output. This approach had the benefit of simplicity, and did not risk the introduction of excessive phase loss that could result from applying a band-pass filter to the sensor signal. The modified algorithm was implemented and functioned as desired. Although the sharp corners of the square wave create an input with high frequency content, the output of the strain rate sensor is dominated by the fundamental bending mode, and so the zero crossings occur at the desired frequency. No repositioning of the sensor was necessary to achieve this result, although sensor orientation is presumably an important factor to the proper operation of the circuit, and may be a subject for further experimentation. Time histories of the output of the strain-rate sensor plotted with the input signal to the actuator when the tuning circuit is engaged are shown in Figure 14 for a system that resonates at 24 Hz. Using a bell-jar apparatus, several experiments have been performed to verify that the closed-loop system tracks the variation in resonant frequency in response to ambient pressure changes.

The control algorithm was implemented using a dSpace™ model DS1005 480 MHz Power PC 750 processor with a model DS2003 16-bit A-to-D converter board and a model DS2103 14-bit D-to-A converter board. The real time process was implemented with a frame rate of 1KHz.

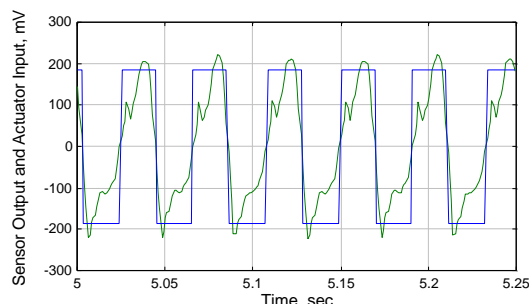


Figure 14. Time histories of strain-rate sensor output and square wave input with tuning circuit engaged.

CONCLUDING REMARKS

Today's fixed-wing MAVs have already demonstrated the potential to function as rapidly deployable autonomous aerial reconnaissance platforms. Such vehicles were confined to the realm of conceptual design only a decade ago, and to the realm of imagination a decade prior to that. Perhaps fifteen years hence, the currently infeasible hummingbird-like MAV concept will enjoy a similar liberation. An extremely agile ornithoptic MAV design would challenge the current state-of-the-art in control for vehicles with highly transient flight characteristics. Developing methods required to model and control a highly agile flapping MAV will promote the understanding of unsteady and nonlinear dynamic phenomena in general, and could generate technologies having broader application to full-scale aircraft.

This work has contributed to an emerging body of multidisciplinary knowledge in the area of biologically inspired micro-scale flight. The research activity seeks to gain and apply an understanding of the function of highly agile natural fliers in the size range of the micro aerial vehicle class. A key factor in this endeavor has been to design and control a vibratory wingbeat apparatus using insights provided by bird, insect, and bat morphologies. Results were presented from a benchtop testbed used to explore a vibratory system that embodied such insights.

A structural concept from an existing MAV design was adapted to create wings having size, weight and planform based on an appropriately scaled hummingbird example. The structure consisted of a carbon-epoxy composite frame covered by a thin layer of latex similar to the battened membrane structure of a bat wing. The wings exhibited a vibratory resonance at the flapping frequency of an equivalently sized hummingbird.

A mechanization concept was developed for a biologically inspired vibratory flapping testbed that provided control over wingtip trajectories generated by the system. A means of varying the testbed actuation signals to generate wingbeat patterns that approximately matched those exhibited by hummingbirds in hover, cruise, and reverse flight was implemented.

A feedback control circuit inspired by locust morphology was also developed and implemented that automatically tunes the actuator drive signal to the resonant flapping frequency of the flexible wing structure. The circuit relies upon a strain-rate feedback signal from a thin film sensor applied to the wing.

ACKNOWLEDGEMENT

Biological insights provided by Dr. Robert Dudley of the Department of Integrative Biology at UC Berkeley are gratefully acknowledged.

REFERENCES

1. Mueller T. J. (editor): Conference on Fixed, Flapping and Rotary Wing Vehicles at Low Reynolds Numbers. Notre Dame University, Indiana, 5-7 June 2000.
2. Dornheim M.A.: Several Micro Air Vehicles in Flight Test Programs. *Aviation Week & Space Technology*, 12 July 1999, pp. 47-48.
3. Grasmeyer J.M., Keennon M.T.: Development of the Black Widow Micro Air Vehicle. AIAA 2001-0127, Aerospace Sciences Meeting, Reno, NV, Jan 2000.
4. Morris, S., Holden, M., "Design of Micro Air Vehicles and Flight Test Validation," Conference on Fixed, Flapping and Rotary Wing Vehicles at Very Low Reynolds Numbers. Notre Dame University, Indiana, 5-7 June 2000.
5. Ifju P.G., Jenkins D.A., Ettinger S., Lian Y., Shyy W.: Flexible-Wing-Based Micro Air Vehicles, AIAA 2002-0705.
6. Ifju, P.G., Ettinger, S., Jenkins, D.A., and Martinez, L., "Composite Materials for Micro Air Vehicles," Society for the Advancement of Materials and Process Engineering Conf., Long Beach, CA, 6-10 May 2001.
7. Waszak, M. R., Jenkins, L. N., and Ifju, P. G., "Stability and Control Properties of an Aeroelastic Fixed Wing Micro Aerial Vehicle," AIAA 2001-4005.
8. Waszak M.R., Davidson J.B., Ifju P.G.: Simulation and Flight Control of an Aeroelastic Fixed Wing Micro Aerial Vehicle. AIAA 2002-4875, AIAA Atmospheric Flight Mechanics Conference, 5-8 August 2002, Monterey, CA.
9. Dudley R., 2000: *The Biomechanics of Insect Flight*. Princeton University Press, Princeton, NJ; ISBN 0-691-04430-9.
10. Dickinson M., 2001: Solving the Mystery of Insect Flight. *Scientific American*, Issue 601, June 2001.
11. Patil, Mayuresh J.: From Fluttering Wings to Flapping Flight: The Energy Connection, AIAA 2001-1460, 42nd AIAA/ASME Structures, Dynamics and Materials Conf., 16-19 April, 2001, Seattle, WA.
12. Yan J., Wood R., Avandhanula S., Sitti M., Fearing R.: Towards Flapping Wing Control for a Micro-mechanical Flying Insect. IEEE International Conference on Robotics and Automation, 2001.
13. Zbikowski R., Pedersen C.B., Hamed A., Friend C.M., Barton, C.P.: Current Research on Flapping Wing Micro Air Vehicles at Shrivenham. AVT Symposium on Unmanned Vehicles for Aerial Ground and Military Operations, Ankara, Turkey, Oct 2000.
14. Boisard T.M., 1998: Preliminary Design Considerations for Micro Air Vehicles: An Approach Based on Hummingbird Flight Characteristics. MS thesis presented to University of Texas at Austin, Dec 1998.
15. Shyy W., Berg M., Ljungqvist D., 1999: Flapping and Flexible Wings for Biological and Micro Vehicles. *Progress in Aerospace Sciences*, v.35, no.5, pp.455-506.
16. Pornsin-Sisirak T., Lee S.W., Nassef H., Grasmeyer J., Tai Y.C., Ho C.M., Keennon M.: MEMS Wing Technology for a Battery-Powered Ornithopter. 13th IEEE International Conference on Micro Electro Mechanical Systems, Miyazaki, Japan, 23-27 Jan 2000.
17. Frampton K.D., Goldfarb M.: Passive Aeroelastic Tailoring for Optimal Flapping Wings. Conference on Fixed, Flapping and Rotary Winged Vehicles for Very Low Reynolds Numbers, Notre Dame, IN, June 2000.
18. Dickinson M. H., Lehmann F., Sane S. P.: Wing Rotation and the Aerodynamic Basis of Insect Flight. *Science*, June 1999, v.284, pp.1954-1960.
19. Schenato L., Deng X., Sastry S.S.: Flight Control System for a Micromechanical Flying Insect: Architecture and Implementation. IEEE International Conference on Robotics and Automation, 2001.
20. Spedding G.R., Lissaman P.B.S., 1998: Technical Aspects of Microscale Flight Systems, *Journal of Avian Biology*, v.29, pp 458-468.
21. Greenwalt C.H., 1960: *Hummingbirds*. Doubleday & Co., Garden City; ISBN 0-486-26431-9.
22. Chai P., Millard D., 1997: Flight and Size Constraints: Hovering Performance of Large Hummingbirds Under Maximal Loading. *Journal of Experimental Biology*, 1997, v.200, pp.921-929.
23. Ennos A.R., 1988: The Importance of Torsion in the Design of Insect Wings. *Journal of Experimental Biology*, v.140, pp.137-160.
24. Cummins J.: Avian Anatomy webpage, April 1 1996, resketched from Freethy R., 1982: *How Birds Work, A Guide to Bird Biology*. 1st ed. Poole: Blanford Press. (<http://numbat.murdoch.edu.au/Anatomy/avian/shoulder1.GIF>)
25. Lasek M., Pietrucha J., Zlocka M., Sibilski K.: Analogies Between Rotary and Flapping Wings from Control Theory Point of View. AIAA 2001-4002, AIAA Atmospheric Flight Mechanics Conference, 6-9 August 2001, Montreal, Canada.
26. Smith, M.J.C.: Simulating Moth Wing Aerodynamics: Towards the Development of Flapping-Wing Technology. *AIAA Journal* v.34, No.7, pp.1348-55, July 1996.
27. Ennos A.R., 1988: The Inertial Cause of Wing Rotation in Diptera. *Journal of Experimental Biology*, v.140, pp.161-169.